Templated Crosslinked Imidazolyl Acrylate for Electronic Detection of Nitroaromatic Explosives

*Hoyoul Kong, Jasmine Sinha, Jia Sun, and Howard E. Katz**

A low-voltage operable, highly sensitive, and selectively responsive polymer for the detection of nitroaromatic explosives is investigated. Resistive devices are fabricated by simple spin-coating on flexible and transparent substrates in addition to silicon substrates and are stable under ambient temperature and oxygen levels before exposure to the nitroaromatics. After exposure to 2,4,6-trinitrotoluene (TNT), the devices show increased conductance, even with picogram (pg) quantities of TNT, accompanied by a confirming color change from colorless to deep red. The relative conductance increase per unit exposure is the highest yet reported for TNT. Aromatic anion salts, on the other hand, do not induce any electronic responses. ^{1}H NMR and microscopic analyses show chemical interactions and morphological changes correlated with the electronic responses, some of which are specific to TNT in relation to other nitroaromatics. The binding constant for the imidazole rings and TNT is on the order of tens of M^{-1}. The materials are promising for rapid indication of exposure to nitroaromatic compounds.

1. Introduction

Sensors for trace detection of explosives have been investigated for environmental remediation and military and homeland defense applications because of terrorist threats.[1,2] Among various nitroaromatic explosives, 2,4,6,-trinitrotoluene (TNT) is the most commonly used.[3,4] In addition, TNT is a poisonous compound that can cause skin irritation and abnormal liver function.[5,6]

Several techniques for detecting TNT have been reported, including mass spectrometry coupled with gas chromatography (GC-MS), ion mobility spectrometry (IMS),[7] microcantilevers,[8] Raman spectroscopy,[5,9,10] X-ray imaging, surface acoustic wave devices,[11] and polymer fluorescence changes.[12] Some of these techniques are very expensive and have limited selectivity, sensitivity, and portability, or require exacting nanofabrication.[13] There are also numerous examples of electrochemical sensing of TNT.[14,15] These demonstrations generally involve highly nanostructured electrodes, rare biomaterials, and/or fluidic electrochemical cells.

Templating, also known in more specific cases as molecular imprinting, has become a widely used method for the preparation of polymeric materials that have the ability to bind a specific chemical species in pores left behind when the template is removed. Three of the above electrochemical examples claim an advantage from templating.[15] In some cases, there have been claims of enhanced geometric specificity to the binding.[2,3,5,9,16,17] Templated polymers are robust, inexpensive, easy to prepare, and have specificity suitable for use in various sensor applications.[17,18] In this work, a commercially derived, lightly crosslinked templated polymer with imidazolyl side chains was found to interact with explosive nitroaromatic compounds such as TNT and 1,3,5-trinitrobenzene (TNB), as well as 2,4- or 2,6-dinitrotoluene (DNT), in a way that leads to increased electrical conductance. While the templating may help ensure that crosslinks could conformationally accommodate guest binding, shape specificity could be limited because of the softness and solubility of the polymer. Regardless of the binding mechanism, responses as a function of time were different for different nitroaromatics, and were easily distinguishable from responses to negatively charged non-nitroaromatic compounds and small molecule solvents, including the aromatic solvent toluene. The active electronic films were fabricated by simple spin coating, and current changes obtained in simple two-terminal tests were hundreds of microamps applying 1–3 V, the highest conductance change yet reported per unit of nitroaromatic exposure. The interaction of the imidazole rings with TNT was characterized by ^{1}H NMR[19] to have a binding constant on the order of tens of M^{-1} in methanol solution. The activity is promising for the detection of nitroaromatic compounds when transferred from nonaqueous or nonpolar platforms, as opposed to electrolyte solutions, and where an electronic signal is particularly desired.

Dr. H. Kong,[+] Dr. J. Sinha, Dr. J. Sun, Prof. H. E. Katz
Johns Hopkins University
Departments of Materials Science
and Engineering and of Chemistry,
3400 North Charles Street, Baltimore, MD 21218, USA
E-mail: hekatz@jhu.edu
[+] Present address: Korea Research Institute of Chemical Technology (KRICT), Ulsan 681-802, Republic of Korea

DOI: 10.1002/adfm.201201711

2. Results and Discussion

2.1. Materials and Testing Procedures

Scheme 1 shows the synthesis, structure, and function of the polymer. The polymer synthesis was carried out using

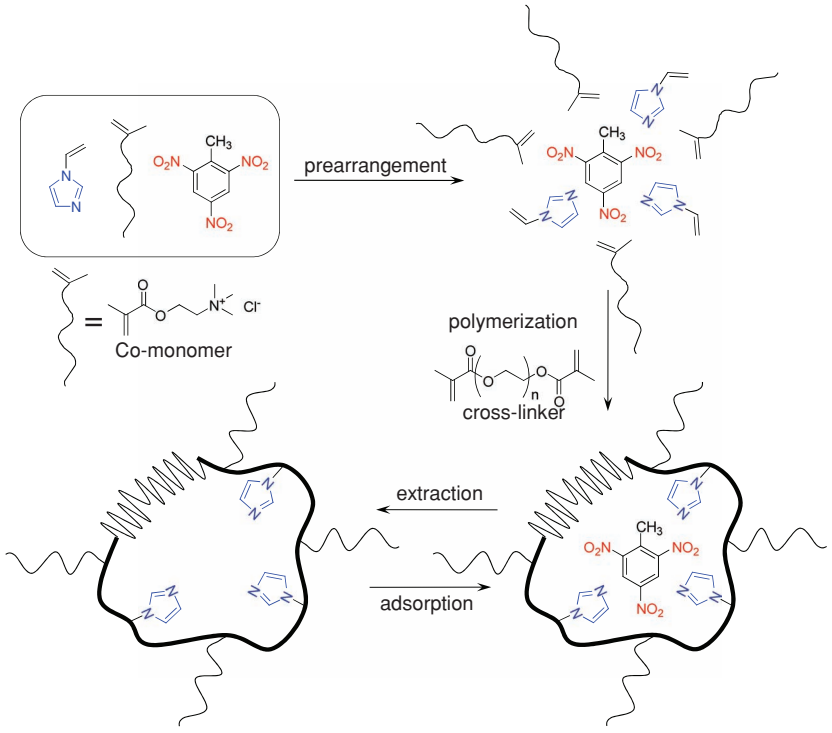

Scheme 1. The reaction scheme and operational principle of the template polymer material.

two different reversible addition fragmentation chain transfer (RAFT) reagents, firstly as reported in a published patent[20] application (trimethylolpropane tris[3-dithiobenzoyloxypropionate] (TMPTDBP)) and secondly using 2-cyanoprop-2-yl-dithiobenzoate (CPDB) as the RAFT reagent in order to verify the generality of the response towards TNT. Monomers undergo copolymerization in the presence of a cross-linker (polyethyleneglycol dimethacrylate (PEGDMA)) and TNT template. Subsequently, the TNT template and low molecular weight compounds are extracted by dialysis. Higher molecular weight, partially networked polymer remains, with free volume and functional groups compatible with nitroaromatics. The polymer was characterized by ^{1}H NMR (see Experimental Section). The M_w for the CPDB polymer was about 3×10^5 g/mol, and the TMPTDBP M_w was about an order of magnitude lower. The differential scanning calorimetry (DSC) thermograms for the polymers did not show any clear peaks indicative of phase transitions from room temperature to 300 °C (Supporting Information Figure S1). UV-vis absorption spectra of the polymer (TMPTDBP) were recorded both in solution and in the film (Supporting Information Figure S2). The UV-vis absorption maxima of the polymer is 227 nm in solution and at even higher energy in film form, essentially transparent in the near UV-vis range. After exposure to some amount of TNT compound, the UV-vis absorption spectra of both polymer solution and film showed newly formed shoulder peaks at 508 nm and 460 nm, respectively.

Polymer films were spin-coated on substrates including stainless steel, Kapton polyimide, and polyethylene terephthalate (PET), in addition to oxide-coated silicon (Si) substrates, and tested with 0.1 to 3 V applied between vapor-deposited interdigitated gold electrodes of total length 2.1 cm, spaced 0.25 mm apart. Polymer films were stable at least on the month time scale (Supporting Information Figure S3). Data were taken with the TMPTDBP polymer, except for comparative data obtained on the CPDB polymer as noted.

The probe station for current–voltage (I–V) measurement was arranged in a relative humidity (RH)-adjustable and temperature-monitored chamber. The baseline current level was RH dependent as shown in **Figure 1**, but stable at any given RH and recoverable on restoration of a prior RH. Sensitivity was greatest at the lowest RH, where the baseline current was lowest. We also found that the hardness and morphology of the polymer film are RH-dependent.

When polar solvents were applied, currents increased: methanol (MeOH) ≫ ethanol (EtOH) > acetonitrile = water ≫ acetone = isopropyl alcohol (IPA) ≫ ethyl acetate > toluene = hexane (Figure 1f). Again, original currents were recovered after solvent evaporation, and these current changes were readily distinguished from those induced by nitroaromatics. We utilized IPA as a solvent vehicle for nitroaromatics because of the modest induced current change by that solvent and the ready miscibility of TNT and the compatibility of the polyacrylate therewith. Responses were essentially instantaneous following analyte application.

2.2. Exposures to Nitroaromatics

The current changes of the polymer (synthesized by using TMPTDBP RAFT reagent) devices after exposure to the TNT in IPA solution and to IPA solvent alone were investigated at various RH (**Figure 2**). The measurements began after stabilization of the RH level. After 1.2 min, 2.5 µL of 1.0 mg TNT/mL IPA solution or IPA itself was dropped on the channel area of the polymer film. In all experiments, the devices exposed to the TNT solution showed much stronger response than those exposed to the pure solvent. Before and after exposure to the TNT, devices measured at higher RH showed much higher absolute current level. Although the absolute current of the devices measured at lower RH was lower, the relative current increase (current after exposure (I)/baseline current before exposure (I_0)) was much larger at lower RH than for those of the devices measured at higher RH, which means the TNT sensitivity is much higher. At very low RH near 1.0%, as soon as the TNT solution was dropped, the current was very rapidly increased from –0.032 µA to –115 µA (about 4000 times), a far greater change than that associated with the solvent. To the best of our knowledge, this is the highest conductance change yet reported in response to a given exposure to an explosive. At RH > 40.4%, immediately when the TNT solution was dropped, the currents were briefly decreased, perhaps because of the lowered water activity, but

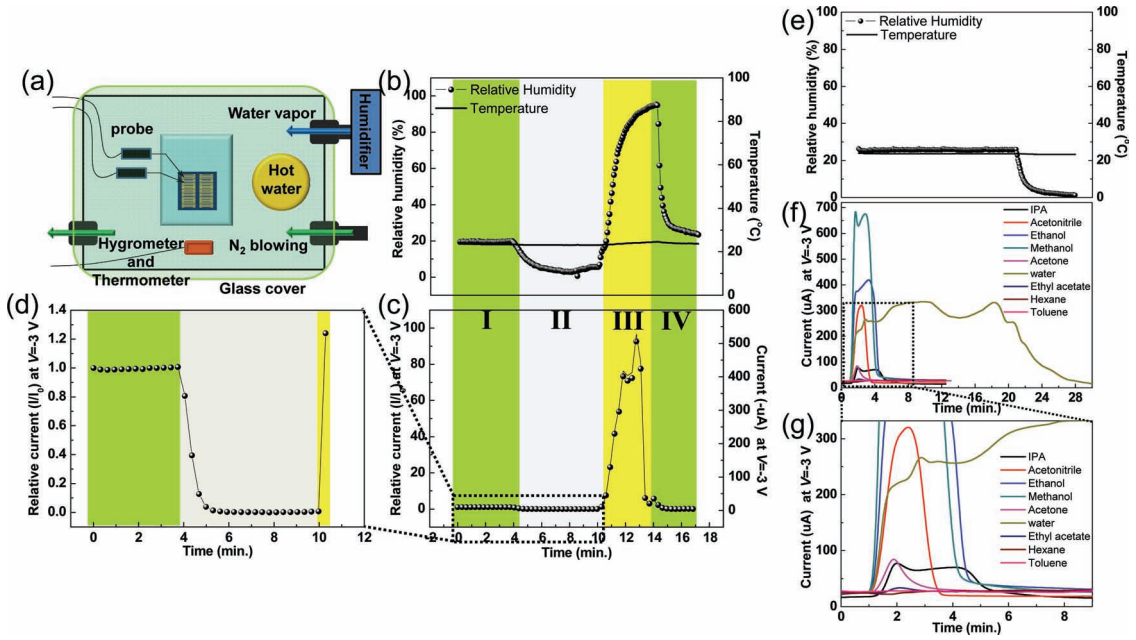

Figure 1. a) Schematic representation for the humidity adjustable probe station setup. b) Constant temperature and relative humidity (RH) changed between 0 and 100% by dry N_2 gas and wet air flow. c) The instant current change of the polymer device from the RH change. d) Enlarged graph of (c) to show near zero current level at 0% RH. e) RH and temperature change for f) the current changes of the devices exposed to various polar and non-polar solvents after 1.0 min and g) enlarged graph of (f).

between 40.0 and 73.0 RH, the TNT-induced current increase was then observed. In addition, the device of the polymer synthesized by using CPDB RAFT reagent also showed similar and reproducible current response to the TNT analyte solution (Supporting Information Figure S4).

We investigated the sensitivity of the TMPTDBP polymer devices using various concentrations of the TNT solutions (**Figure 3**a). Consistent current changes were observed. At higher TNT concentrations, the initial current change was much larger. In contrast, at lower TNT concentrations, although the initial current signal was much lower, the current was eventually increased over a longer time.

Devices exposed to TNT were investigated at various voltages from –3.0 to –0.1 V versus a grounded electrode (Figure 3b,c). Detection was accomplished at all voltages in the range, and at lower voltage, the time of elevated current was longer.

We tested the films on flexible or transparent substrates such as stainless steel, PET film, and Kapton film (Figure 3d). The substrates were used without any surface treatments or special cleaning except for air blowing for removing dust. All devices showed current changes similar to what was observed on Si substrates. The PET film with polymer layer was flexible and transparent. After exposure to the TNT analyte, the transparent PET film became obviously red.

To investigate how long the polymer devices can be stored before attempting TNT detection, we fabricated multiple devices at the same time, and measured each device exposed to the TNT analyte after different storage times at 17% RH. The current change after exposure to the TNT analyte was reproducible (Supporting Information Figure S5).

The reactivity of the devices to a series of nitroaromatics including TNT, 1,3,5-TNB, 2,4-DNT, 2,6-DNT, and 4-amino-2,6-DNT, were investigated (Figure 3e–g). The apparent morphological change of the polymer film was observed by optical microscopy only with TNT exposure. In addition, we investigated the electrical changes using solution concentration levels of 1.0 and 0.01 mg nitroaromatics/mL IPA. TNT gave one of the strongest initial responses, with other nitroaromatics showing similar or less initial response. Devices exposed to TNT showed more sharply dropped current after the peaks at the higher concentration. Thus, the polymer detects nitroaromatics in general, with TNT giving a distinct current evolution at the higher concentration. The polymer devices exposed to negatively charged aromatic salts such as sodium benzoate and sodium benzenesulfonate were also investigated. Although these aromatic anions have similar molecular shape and size compared to nitroaromatic explosives, there was no distinct current response, and no morphological or color changes when the polymer devices were exposed to the non-nitroaromatic compounds, in contrast to that observed for nitroaromatic explosives (Supporting Information Figure S6).

To investigate the effect of the polymer thickness on the TNT sensitivity, many devices with a variety of thicknesses (0.9 to 24.1 μm) were prepared with different casting methods (spin or drop) using different concentration of the polymer solution (5 to 30%) (Supporting Information Figure S7). The device with thinner polymer film showed larger relative current increase after exposure to TNT analyte. The polymer device with 0.9 μm thickness film exposed to 2.5 μL of 1.0 mg TNT/mL IPA showed 83 000 times increased current.

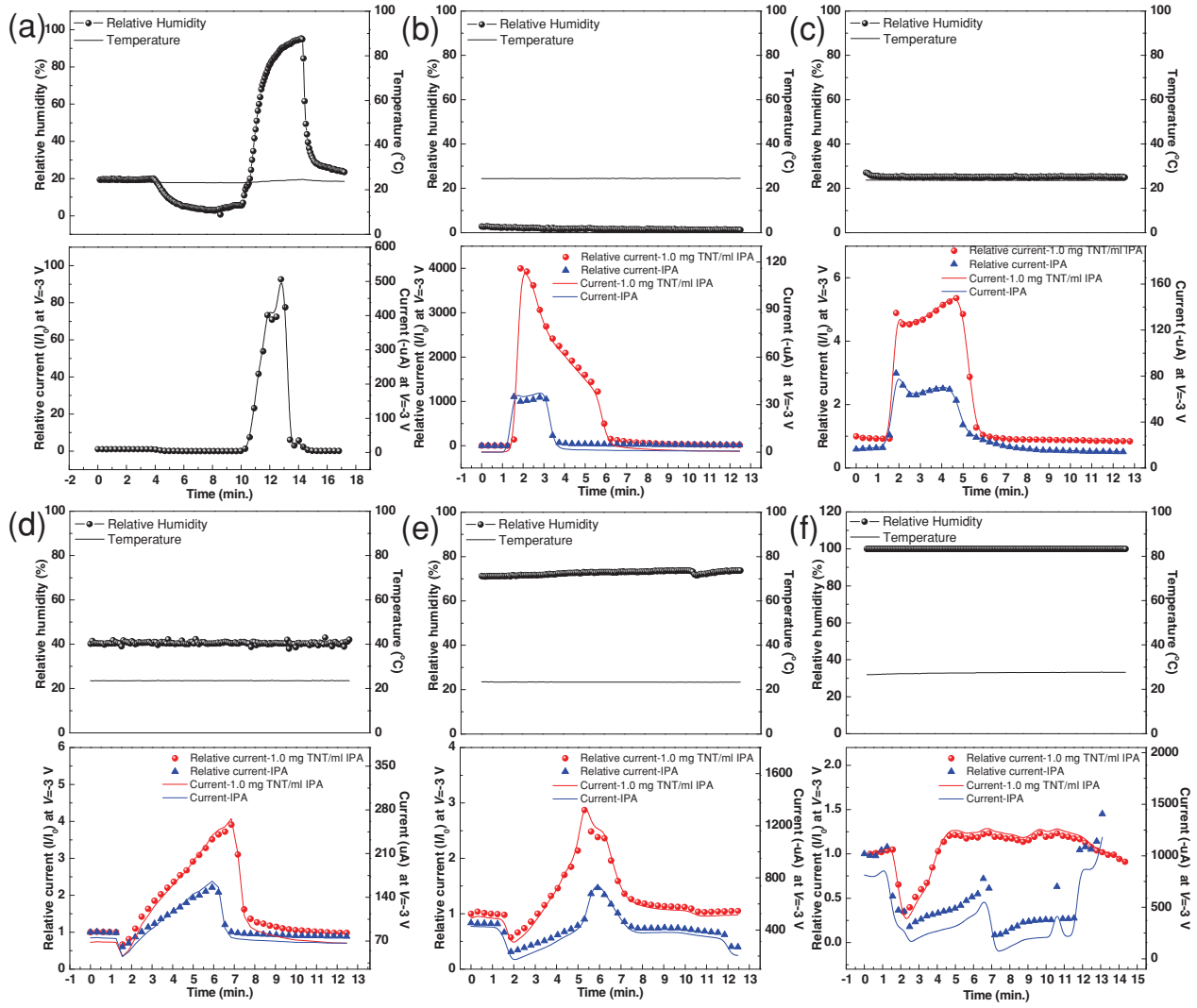

Figure 2. a) The current change of the polymer device caused by RH changes. b–f) Current changes of the devices exposed to 2.5 µL of 1.0 mg TNT/mL IPA solution and pure IPA solvent after 1.2 min at near b) 1.0%, c) 25.0%, d) 40.0%, e) 73.0%, and f) 100.0% RH conditions. Note different *y*-axes. In all panels the top panels show the RH and temperature and the bottom panels show the current changes.

We repeatedly dropped TNT solution of various concentrations four times on the same probed area of each polymer device (**Figure 4**). The device exposed to higher concentration TNT solution showed much more increased current from the first drop of TNT solution than from subsequent drops. On the other hand, when the IPA solvent was dropped several times on the same channel area, very similar current changes were reproduced. When the much lower-concentration TNT solution was dropped, the repeated similar current change was observed as for the IPA drop. These results show that the binding of TNT is stable and saturable, even inhibiting the response to the solvent alone. The decreased response for later TNT drops does not reflect a lack of polymer response, but simply the existence of a finite number of active sites that eventually become occupied. This is a possible consequence of the template-induced arrangement of the polymer crosslinks.

2.3. TNT-Induced Morphology Changes

Figure 5 shows the surface images of films, which had been previously tested electrically, exposed to TNT solution or IPA solvent. The film morphology from a device exposed to the IPA solvent was not changed compared to the initial film. In contrast, when the film was exposed to TNT solution, clearly changed surface images were observed, caused by the reaction mentioned above. In addition, the surface images of the film over time after exposure to the TNT solution or IPA solvent were observed for 10 min (Supporting Information Figure S8). In the case of the IPA drop, there was no change except for solvent evaporation. However, in the case of the TNT solution drop, we can see the clear formation and movement of domains which were reacted with TNT analyte.

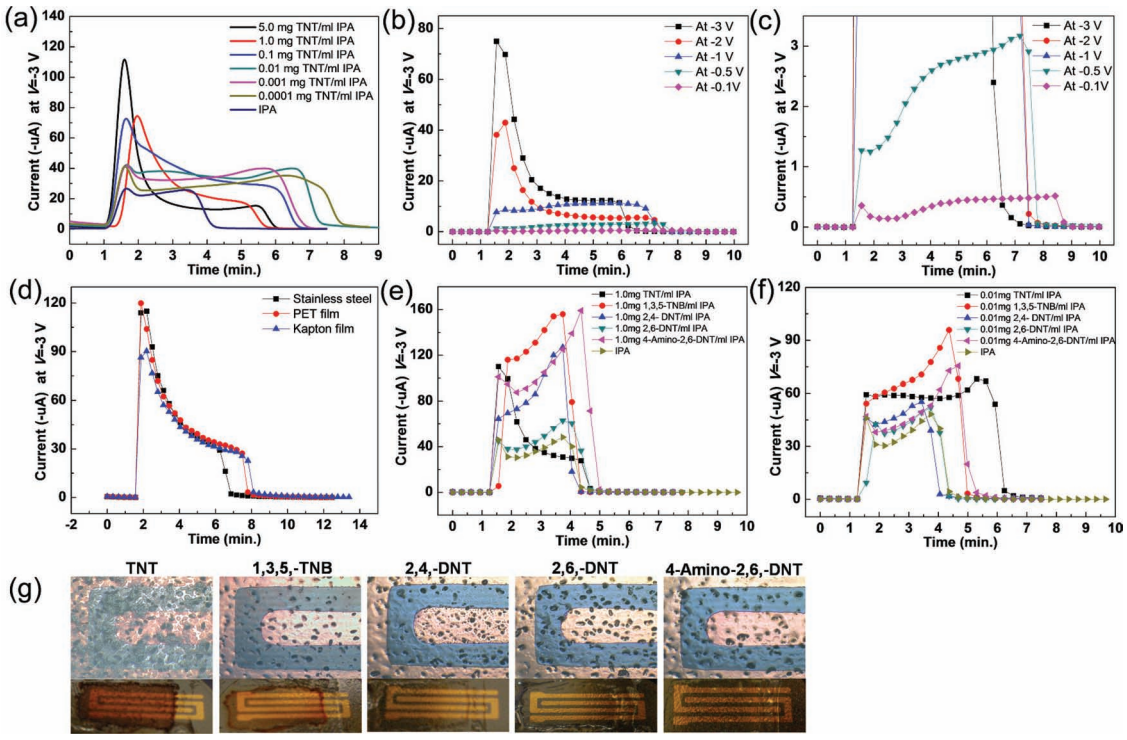

Figure 3. a) Sensitivity of the polymer devices using TNT solutions of various concentrations near 0% RH: current changes of devices exposed to the various concentrations. b) Very low-voltage (–0.1 V) operable devices and c) an enlarged graph of (b). d) Devices on the flexible or transparent substrates such as stainless steel, PET, and Kapton film. e) 1.0 and f) 0.01 mg nitroaromatics/mL IPA after 1.2 min. g) Upper panels: optical microscopy images and lower panels: pictures of devices that were used for (e).

To obtain atomic force microscopy (AFM) images, 5.0 µL TNT solution or IPA solvent was dropped on the polymer film which had been spincast on a silicon substrate (Supporting Information Figure S9,S10). The sample exposed to the IPA solvent showed very similar surface morphology to that of the initial film, including very large crystal domains. However, after exposure to the TNT solution, the film showed a periodic wavy structure with average depth about 4 nm.

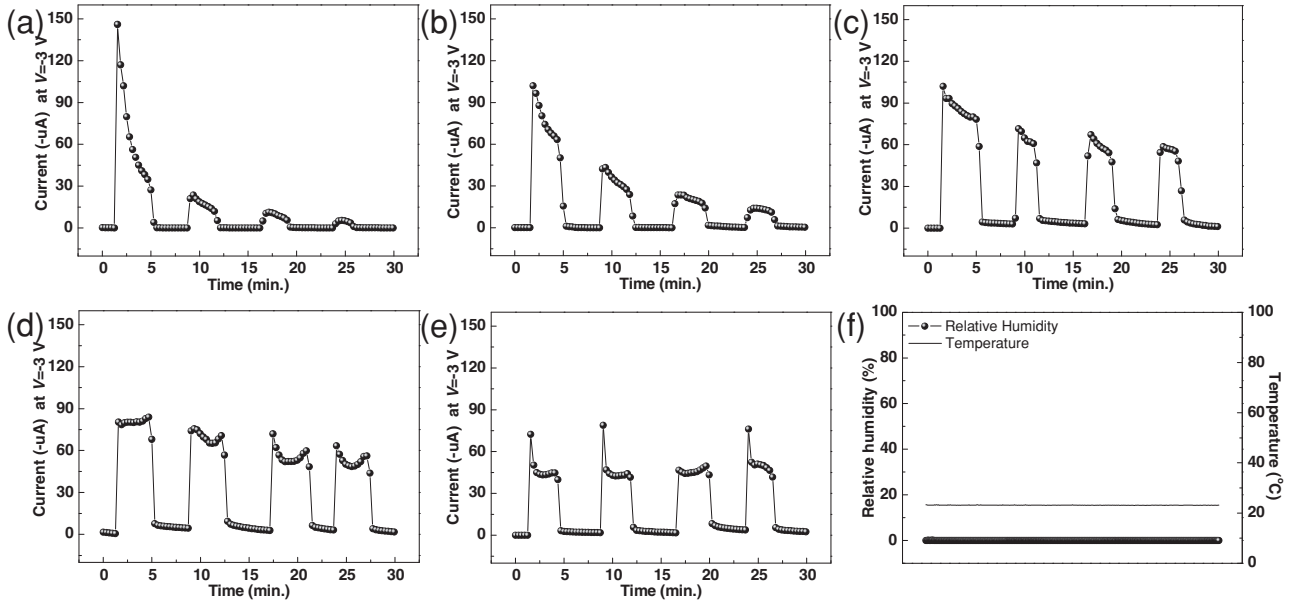

Figure 4. Current responses to 2.5 µL TNT solutions of various concentrations a) 1.0, b) 0.5, c) 0.1, and d) 0.05 mg/mL IPA and e) IPA solvent dropped 4 times on the same probed area of each polymer device. f) The constant 0% RH and temperature.

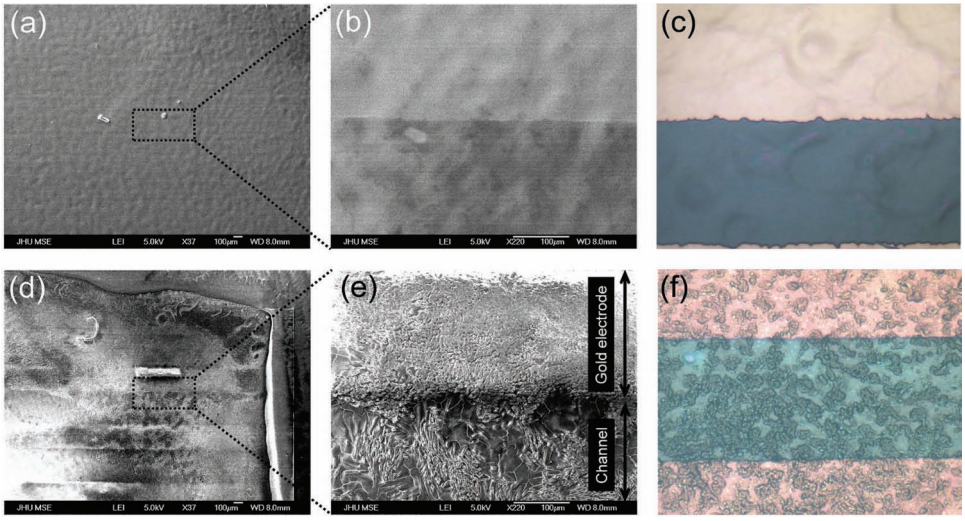

Figure 5. a,b,d,e) Scanning electron microscopy (SEM) and c,f) optical microscopy images of the polymer devices exposed to the IPA (a–c) and TNT solutions (d–f).

We additionally measured the X-ray diffraction (XRD) of the polymer films before and after dropping TNT solution or IPA alone in order to see the changes in the microstructure. We confirmed that the same crystalline peaks were retained after dropping IPA alone, but, after exposure to the TNT analyte, the film became nearly amorphous (Supporting Information Figure S11).

2.4. NMR Studies and Reaction Mechanism

There are two possible types of reactions that could cause these various physical changes. The imidazole groups may interact with TNT through various types of non-covalent bonding mechanisms, including hydrophilic/hydrophobic, electrostatic, hydrogen bonding, and van der Waals forces. Covalent chemistry is also possible (Supporting Information Figure S12): the imidazole functional groups have pKa values in the range of 6.0–9.0, basic enough to deprotonate the methyl group of TNT or form a Meisenheimer complex with nitroaromatics.

Evidence of these reactions was obtained from ^{1}H NMR of polymer solutions before and after adding some amount of the TNT analyte (**Figure 6**). We dissolved the solid polymer resin and TNT in CD_3OD. Before TNT addition, the imidazole peaks clearly split and the solution color was transparent. As soon as a very small amount of TNT solution (0.01 mL, at the threshold for observation of a distinct TNT peak) was added, the color was very rapidly changed to dark red, the 7.8 ppm imidazole peak was slightly broadened, and all peaks were shifted upfield. When 0.1 mL of TNT solution was added, a broad TNT peak was observed. As more TNT solution was added to the polymer solution, the imidazole peaks were much more broadened and diminished, and shifted further upfield. When a small amount of polymer solution was added to a TNT solution, very similar peak changes were observed. These results verify the strong chemical interactions hypothesized between imidazole groups and TNT in the material.

We quantified these interactions by ^{1}H NMR titration as follows. We added increasing amounts of predissolved TNT to achieve a range of concentrations of 0 to 0.092 M in a second solution that originally contained 300 mg of polymer in 0.6 mL of CD_3OD. The concentration of imidazole groups in the solution was calculated by relative integration of the imidazole protons compared to the TNT protons, whose concentration was known. The total concentration of free plus complexed imidazole groups decreased as more and more TNT solution was added. The complexation-induced shifts ($\triangle\delta$) of the TNT aryl proton (**Figure 7**) were monitored and the binding constant for the interaction between the host and analyte was calculated,[19] assuming that there is a 1:1 binding isotherm, using Equation 1.

$$K = [C]/([T][M]) \quad (1)$$

where $[T] = [T]_t - [C]$ and $[C] = [T]_t [(\delta-\delta_t)/(\delta_c-\delta_t)]$. $[T]_t$ is the total concentration of added TNT, [C] is the concentration of the complex after equilibration, [T] is the concentration of the free TNT after equilibration, [M] is the concentration of free imidazole moieties in the polymer at equilibrium, δ is the observed TNT ^{1}H chemical shift, and δ_t and δ_c are the chemical shifts of TNT in free and totally complexed forms, respectively. δ_c was observed either as the onset of the left side of the aryl proton (H_T) peak on TNT, or by extrapolation to a single value at zero TNT concentration. With the increase in the concentration of TNT, δ moves upfield; this shielding of H_T leads us to conclude that the imidazole forms an adduct with TNT molecule, which is plausibly a Meisenheimer complex, as shown in Figure 7A (inset). Further addition of TNT makes δ move more towards pure TNT, which is presumably due to the increased weighting of the concentration of free TNT.

The binding constant K for the interaction between the imidazole on the polymer and the TNT was found to be 53 M^{-1} with a standard deviation of 8 M^{-1} arising from nonsystematic uncertainty, when the "onset" method was used to calculate δ_c. When various extrapolations to a single value of δ_c were used, K between 20 and 60 was obtained, but the error was systematic; higher values were obtained at the lowest TNT concentrations.

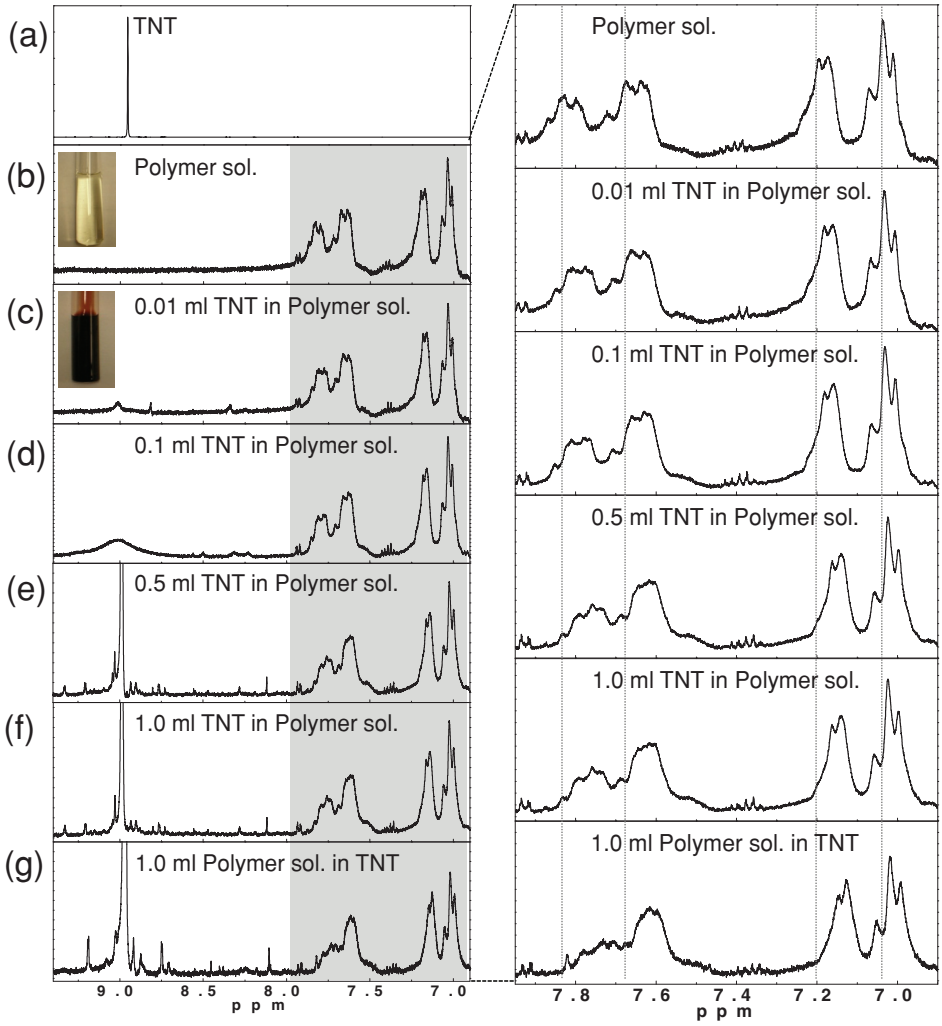

Figure 6. NMR spectroscopy (^{1}H aromatic region) of a) TNT and b) polymer solution. c) 0.01, d) 0.1, e) 0.5, and f) 1.0 mL TNT solution added to the polymer solution of (b) and g) 1.0 mL polymer solution added to TNT solution of (a).

The listing of data on which these calculations are based is given in the Supporting Information. If an extrapolation method is deemed more appropriate, then the data would indicate a suppression of TNT activity at higher concentrations, perhaps from self- or nonspecific aggregation. The "onset" method seems to internally correct for these effects. The binding constant, while modest for dilute solutions, is ample for TNT-imidazole binding and response when little or no solvent is present in an imidazole-rich (0.1 M), low-volume (0.1 μL = 1 μm × 1 cm^2) polymer film, in which case the TNT and imidazole groups are each approximately 50% complexed under the conditions of our experiment.

3. Conclusions

The interaction between TNT and imidazole groups bound to a crosslinked acrylate polymer was found for the first time to cause an increase in conductivity of the polymer, along with the expected color change. Other nitroaromatics also caused related but distinct time-dependent conductivity changes in contrast to that observed for negatively charged non-nitroaromatic compounds. Morphological changes in the polymer were observed as well. The TNT-imidazole binding phenomenon was observed for a concentrated solution of the polymer in CD_3OD using NMR spectroscopy, and an equilibrium binding constant on the order of 20–60 M^{-1} was determined, showing the favorability of the association.

4. Experimental Section

Synthetic Procedures: Acrylate polymers were prepared according to a reported procedure,[20] which is summarized here. The preparation used *N*-vinylimidazole (25 mg, 5%) as a preformed salt with TNT, trimethylammonium ethylmethacrylate chloride (TMAMA, ≈400 mg) to increase solubility in polar solvents, and poly(ethylene glycol) dimethacrylate (PEGDMA) (MW 550, 25 mg, 5%) as a cross-linker in the presence of the RAFT reagents (TMPTDBP or CPDB) (20 mg). The polymerization reaction was carried in a sealed tube with dimethylsulfoxide (DMSO, 2 mL) as solvent and 2,2′-azobisisobutyronitrile (AIBN) (1%)

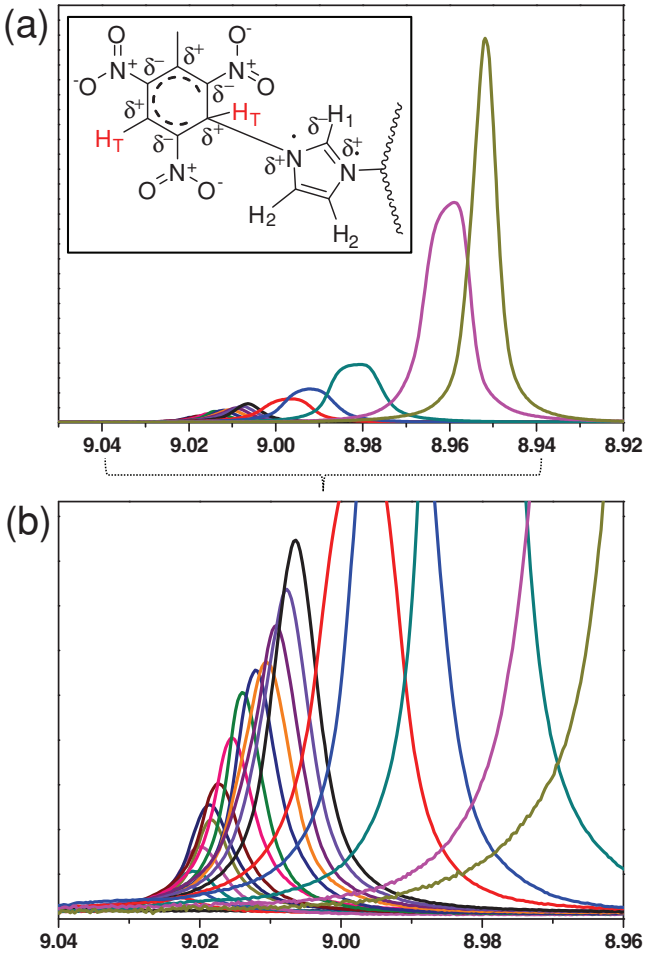

Figure 7. a) ^{1}H NMR titration spectra showing TNT (0–0.092 M) aryl proton (H_T) shift on increasing its concentration in polymer solution in CD_3OD. Inset: Proposed complex formation of TNT with imidazoles attached to the polymer. Note the assigned chemical shift changes on complexation, consistent with our NMR observations. b) Expanded view of ^{1}H NMR titration spectra.

as catalyst. The mixture was heated at 70–80 °C for 4 h to promote polymerization. For purification of the polymer, the reaction mixture was dialyzed (MW cutoff of 3500) against water. For template removal, the polymer solution was further dialyzed against a sodium bicarbonate buffer and aqueous ammonium solutions. ^{1}H NMR of the polymer using TMPTDBP (CD_3OD, δ ppm): 1.25, 1.67, 1.88, 2.29, 3.38, 3.44, 3.59, 3.66, 4.02, 4.12, 7.02, 7.27, 7.62, 7.80, 7.93.

^{1}H NMR of the polymer using CPDB (CD_3CN, δ ppm): 0.88, 1.27, 1.53, 1.62, 1.76, 3.02, 3.55, 3.68, 4.18, 4.23, 5.6, 6.02, 6.8, 7.14, 7.56, 7.62, 7.71, 7.94.

Measurements: ^{1}H NMR spectra were recorded on a Bruker AVANCE 400 MHz spectrometer, with Me_4Si as an internal reference. The weight average molar mass (M_w) of the MIPs was determined using SLS (DAWN-HELEOS-II, Wyatt Technology) equipped with a laser operating at 658 nm. The measurements were carried out in water or acetonitrile at 22 °C. The d*n*/d*c* were determined using Optilab T-rex at 658 nm. DSC measurement was performed using a TA Q20 instrument under a nitrogen atmosphere at a heating rate of 5 °C/min. The UV-vis spectra were recorded using a Cary 50 UV-vis spectrometer. The AFM measurements were performed in tapping mode with a Pico Plus scanning probe microscope. XRD measurements were carried out on a Phillips X-pert pro X-ray diffraction system. The polymer film thickness was measured by using SLOAN DEKTAK II.

Fabrication and Characterization of Chemoresistors: Heavily n-type doped silicon wafers with 100 nm of thermally grown silicon dioxide layers were used as substrates. Wafers were cleaned by sonication in acetone and IPA. In addition, we also used flexible or transparent substrates such as stainless steel, PET, and Kapton films after air-blowing to remove dust. Gold electrodes were evaporated through a shadow mask. Polymer solution was spin coated at 1500 rpm for 60 s on the substrates with gold electrodes. Films were annealed at 60 °C for removing methanol solvent. All the current–voltage (*I*–*V*) curves of devices were measured with an Agilent 4155C. The polymer devices were measured at –3 to +3 V, and the current at –3 V was extracted and plotted to show the current change (before and after exposure to analytes) versus time. For measuring, the temperature was maintained at constant values and the humidity was controlled by a humidifier and dry N_2 gas flow.

Supporting Information

Supporting Information is available from the Wiley Online Library or from the author.

Acknowledgements

H.K. and J.S. contributed equally to this work. The authors thank S. Kola, M. Yeh, and B. Zhang for contributions to physical and chemical characterizations. This work was partially funded by Raptordetection LLC, who also supplied the (TMPTDBP)) polymer material and provided helpful technical interactions.

Received: June 24, 2012
Published online: August 13, 2012

[1] a) E. S. Snow, F. K. Perkins, E. J. Houser, S. C. Badescu, T. L. Reinecke, *Science* **2005**, *307*, 1942; b) M. E. Germain, M. J. Knapp, *Chem. Soc. Rev.* **2009**, 2543.
[2] M. Riskin, R. Tel-Vered, T. Bourenko, E. Granot, I. Willner, *J. Am. Chem. Soc.* **2008**, *130*, 9726.
[3] N. R. Walker, M. J. Linman, M. M. Timmers, S. L. Dean, C. M. Burkett, J. a. Lloyd, J. D. Keelor, B. M. Baughman, P. L. Edmiston, *Anal. Chim. Acta* **2007**, *593*, 82.
[4] K. D. Smith, B. R. McCord, W. A. MacCrehan, K. Mount, W. F. Rowe, *J. Forensic Sci.* **1999**, *44*, 789.
[5] L. Yang, L. Ma, G. Chen, J. Liu, Z.-Q. Tian, *Chem. Eur. J.* **2010**, *16*, 12683.
[6] J. Hawari, S. Beaudet, A. Halasz, S. Thiboutot, G. Ampleman, *Appl. Microbiol. Biotechnol.* **2000**, *54*, 605.
[7] a) R. G. Ewing, D. A. Atkinson, G. A. Eiceman, G. J. Ewing, *Talanta* **2001**, *54*, 515; b) G. R. Asbury, J. Klasmeier, H. H. Hill, *Talanta* **2000**, *50*, 1291.
[8] a) P. G. Datskos, N. V. Lavrik, M. J. Sepaniak, *Sens. Lett.* **2003**, *1*, 25; b) L. A. Pinnaduwage, A. Wig, D. L. Hedden, A. Gehl, D. Yi, T. Thundat, R. T. Lareau, *J. Appl. Phys.* **2004**, *95*, 5871; c) L. A. Pinnaduwage, D. Yi, F. Tian, T. Thundat, R. T. Lareau, *Langmuir* **2004**, *20*, 2690.
[9] E. L. Holthoff, D. N. Stratis-Cullum, M. E. Hankus, *Sensors* **2011**, *11*, 2700.
[10] a) E. M. A. Ali, H. G. M. Edwards, I. J. Scowen, *J. Raman Spectrosc.* **2009**, *40*, 2009; b) L. C. Pacheco-Londono, W. Ortiz-Rivera, O. M. Primera-Pedrozo, S. P. Hernandez-Rivera, *Anal. Bioanal. Chem.* **2009**, *395*, 323.

[11] X. G. Yang, X. X. Du, J. X. Shi, B. Swanson, *Talanta* **2001**, *54*, 439.
[12] a) C. J. Cumming, C. Aker, M. Fisher, M. Fox, M. J. la Grone, D. Reust, M. G. Rockley, T. M. Swager, E. Towers, V. Williams, *IEEE Trans. Geosci. Remote* **2001**, *39*, 1119; b) A. Rose, C. G. Lugmair, T. M. Swager, *J. Am. Chem. Soc.* **2001**, *123*, 11298; c) S. Yamaguchi, T. M. Swager, *J. Am. Chem. Soc.* **2001**, *123*, 12087; d) S. Zahn, T. M. Swager, *Angew. Chem. Int. Ed.* **2002**, *41*, 4225; e) A. Rose, Z. G. Zhu, C. F. Madigan, T. M. Swager, V. Bulovic, *Nature* **2005**, *434*, 876; f) H. Sohn, R. M. Calhoun, M. J. Sailor, W. C. Trogler, *Angew. Chem. Int. Ed.* **2001**, *40*, 2104; g) H. Sohn, M. J. Sailor, D. Magde, W. C. Trogler, *J. Am. Chem. Soc.* **2003**, *125*, 3821; h) S. J. Toal, D. Magde, W. C. Trogler, *Chem. Commun.* **2005**, 5465; i) A. Narayanan, O. P. Varnavski, T. M. Swager, T. Goodson, *J. Phys. Chem. C* **2008**, *112*, 881.
[13] J. Huang, T. J. Dawidczyk, B. J. Jung, J. Sun, a. F. Mason, H. E. Katz, *J. Mater. Chem.* **2010**, *20*, 2644.
[14] a) A. D. Aguilar, E. S. Forzani, M. Leright, F. Tsow, A. Cagan, R. A. Iglesias, L. A. Nagahara, I. Amlani, R. Tsui, N. J. Tao, *Nano Lett.* **2010**, *10*, 380; b) P. C. Chen, S. Sukcharoenchoke, K. Ryu, L. G. de Arco, A. Badmaev, C. Wang, C. W. Zhou, *Adv. Mater.* **2010**, *22*, 1900; c) W. Chen, Y. Wang, C. Bruckner, C. M. Li, Y. Lei, *Sens. Actuators B* **2010**, *147*, 191; d) Y. Engel, R. Elnathan, A. Pevzner, G. Davidi, E. Flaxer, F. Patolsky, *Angew. Chem. Int. Ed.* **2010**, *49*, 6830; e) S. J. Guo, D. Wen, Y. M. Zhai, S. J. Dong, E. K. Wang, *Biosens. Bioelectron.* **2011**, *26*, 3475; f) J. Jaworski, K. Yokoyama, C. Zueger, W. J. Chung, S. W. Lee, A. Majumdar, *Langmuir* **2011**, *27*, 3180; g) T. H. Kim, B. Y. Lee, J. Jaworski, K. Yokoyama, W. J. Chung, E. Wang, S. Hong, A. Majumdar, S. W. Lee, *ACS Nano* **2011**, *5*, 2824; h) Y. X. Liu, D. Lan, W. Z. Wei, *J. Electroanal. Chem.* **2009**, *637*, 1.
[15] a) T. Alizadeh, M. Zare, M. R. Ganjali, P. Norouzi, B. Tavana, *Biosens. Bioelectron.* **2010**, *25*, 1166; b) D. C. Apodaca, R. B. Pernites, F. R. Del Mundo, R. C. Advincula, *Langmuir* **2011**, *27*, 6768; c) D. X. Nie, D. W. Jiang, D. Zhang, Y. Liang, Y. Xue, T. S. Zhou, L. T. Jin, G. Y. Shi, *Sens. Actuators B* **2011**, *156*, 43.
[16] a) B. R. Hart, K. J. Shea, *Encyclopedia of Polymer Science and Technology*, Wiley, New York **2002**; b) G. E. Southard, G. M. Murray, *Recognit. Recept. Biosens. Part 3* **2010**, 751; c) A. McCluskey, C. I. Holdsworth, M. C. Bowyer, *Org. Biomol. Chem.* **2007**, *5*, 3233; d) J. Li, C. E. Kendig, E. E. Nesterov, *J. Am. Chem. Soc.* **2007**, *129*, 15911; e) R. C. Stringer, S. Gangopadhyay, S. A. Grant, *Anal. Chem.* **2010**, *82*, 4015; f) G. Bunte, J. Hürttlen, H. Pontius, K. Hartlieb, H. Krause, *Anal. Chim. Acta* **2007**, *591*, 49.
[17] M. J. Whitcombe, I. Chianella, L. Larcombe, S. A. Piletsky, J. Noble, R. Porter, A. Horgan, *Chem. Soc. Rev.* **2011**, *40*, 1547.
[18] a) S. A. Piletsky, E. V. Piletskaya, T. L. Panasyuk, A. V. El'skaya, R. Levi, I. Karube, G. Wulff, *Macromolecules* **1998**, *31*, 2137; b) A. L. Jenkins, O. M. Uy, G. M. Murray, *Anal. Chem.* **1999**, *71*, 373.
[19] K. Hirose, *J. Incl. Phenom. Macrocyclic Chem.* **2001**, *39*, 193.
[20] A. Kalivretenos, K. V. Houten, J. Gluckman, F. Hardy, I. Dorovskoy, R. Trower, *WO/2010/078426*, World Patent, **2010**.